Journal of Applied Polymer Science

Thin Dense Films from Polymer Blend of Thermoplastic Elastomer and Polyolefin by Uniaxial Stretching

Masamoto Uenishi,[1*] Noriaki Fukushima,[1†] Masashi Teramachi,[1*] Masahiko Mizuta,[1*] Jun Kamo,[1‡] Toshinori Tsuru[2]

[1]Corporate Research Laboratories, Mitsubishi Rayon Co., Ltd., Ohtake, Hiroshima 739-0093, Japan

[2]Department of Chemical Engineering, Hiroshima University, Higashi-Hiroshima, Hiroshima 739-8527, Japan

*Present address: Toyohashi Corporate Research Laboratories, Mitsubishi Rayon Co., Ltd., 4-1-2 Ushikawa-Dohri, Toyohashi, Aichi 440-8601, Japan.

†Present address: Head Office, Mitsubishi Rayon Co., Ltd., 6-41, Konan 1-chome, Minato-ku, Tokyo 108-8506, Japan.

‡Present address: Graduate School of Engineering, Nagasaki University, 1-14 Bunkyo, Nagasaki 852-8521, Japan.

Correspondence to: M. Uenishi (E-mail: uenishi_ma@mrc.co.jp)

ABSTRACT: Thin dense films composed of a thermoplastic elastomer [polystyrene-block-poly(ethylene butylene)-block-polystyrene triblock copolymer (SEBS)] and two polyolefins, poly(ethylene-*co*-ethylacrylate) and poly(ethylene-*co*-propylene), were obtained by blow molding, uniaxial hot stretching, and cooling to room temperature. In the resulting films, the dispersed polyolefin phase formed a 3D-network structure which constrained the elastic recovery of the SEBS matrix phase. The presence of this network structure was a key factor in forming the thin dense films. © 2012 Wiley Periodicals, Inc. J. Appl. Polym. Sci. 000: 000–000, 2012

KEYWORDS: membranes; morphology; blends; polyolefins; thermoplastics

Received 5 May 2012; accepted 19 July 2012; published online
DOI: 10.1002/app.38379

INTRODUCTION

Recently, submicron fabrication methods for line and space patterns in semiconductor manufacturing have been developed using photolithography techniques. In this semiconductor manufacturing process, prevention of small defects is very important, because such defects lower the product yield rate.[1] If small bubbles occur in the chemical liquids (e.g., isopropyl alcohol (IPA), photoresist polymer solution, developer solution) used in the manufacturing process, this leads to the formation of defects.

To remove such bubbles, a separation method using a thin dense highly gas permeable membrane can be applied. However, if a porous membrane is used, the liquid can pass through the pores and its concentration becomes changed. For this reason, porous membranes are not suitable for this purpose.

Thermoplastic polymers with high gas permeability, flexibility, and chemical resistance to the typical chemical liquids above are preferable for use as degassing membrane materials. The purpose of the present study was to develop a method of producing thin dense films from the gas permeable thermoplastic polymer materials using melt-extrusion and stretching process without solvent. This process would give low stress on environment. Table I shows the melt flow rate (MFR) and gas permeability for typical thermoplastic polymer materials.

Thermoplastic elastomers and polyolefins are the candidate materials currently being considered because of their good resistance to liquid chemicals.[10] Using the thermoplastic elastomer SEBS [polystyrene-block-poly(ethylene butylene)-block-polystyrene triblock copolymer], thin films can be produced by hot pressing and stretching at temperatures significantly higher than the glass transition temperature of the polystyrene domains. However, upon cooling to room temperature, physical crosslinking of the polystyrene domains reoccurs, leading to elastic recovery and a return to the original thickness.[11,12] For this reason, thin films of this thermoplastic elastomer are difficult to produce. In contrast, for polyolefin, thin dense films can be obtained by a melt-extrusion and stretching process. However, the gas permeability of the stretched film becomes very low as the amount of stretching is increased because the crystallinity increases and the mobility of the amorphous chain decreases.[13,14]

We propose the formation of a thin dense membrane by appropriate control of the morphology of a polymer blend consisting of both a thermoplastic elastomer and a polyolefin, allowing the shortcomings of each to be mutually overcome. The concept behind this type of morphology control is shown in Figure 1. In this example, the morphology corresponds to that produced by blow molding, uniaxial stretching, and cooling. The

Table I. Melt Flow Rate (MFR) and Gas Permeability for Typical Thermoplastic Polymer Materials

Thermoplastic polymer materials		Trade name	MFR[a]	Gas permeability[b]			Ref.
				O_2	N_2	O_2/N_2	
Thermoplastic elastomer	SEBS	KRATON G1652[c]	No flow[d]	22.0[e]	7.7[e]	2.9[e]	2, 3
	Hydrogenated polybutadiene[f]			11.3	4.0	2.8	4-6
Polyolefin	Polyethylene[g]		1.7	2.9	1.0	2.9	4-6
	Polypropylene			2.3[h]	0.4[h]	5.1[h]	4, 5, 7
	Ethylene-ethylacrylate copolymer	NUC6170[i]	6.0	8.2	2.9	2.8	9
Others	Polystyrene[j]			2.6	0.8	3.3	4, 5, 8

[a]Units g/10 min at 190°C 2.16 kg load, [b]Units 10^{-10} cm^3 (25°C) cm cm^{-2} s^{-1} (cm Hg)$^{-1}$, [c]Products of Kraton Polymers LLC, [d]200°C, 5 kg load, [e]Film cast from polymer solution by authors, [f]Ethylene butylene copolymer, crystallinity 29%, [g]Low density polyethylene, [h]Data at 30°C, [i]NUC6170 is a product by Nippon Unicar (Japan), [j]Biaxially oriented film.

thermoplastic elastomer is assumed to be SEBS. As shown in Figure 1(a), the as-blown annealed film consists of a dispersed fibril phase of polyolefin and a SEBS matrix phase. The SEBS matrix is also phase-separated into polystyrene domains that act as the crosslink points and poly(ethylene-butylene) chains.[11,12] Figure 1(b) shows the stretched film (melt state) under uniaxial hot stretching in the machine direction (MD). In this process, the crosslinking polystyrene domains melt and the entire SEBS matrix phase becomes stretched. The dispersed fibril phase also melts and is stretched. As the stretching ratio increases, the thickness of the film decreases. In addition, the distance between neighboring fibrils decreases in the thickness direction and these fibrils eventually become stacked above each other. This stacked fibril phase forms a network-like structure that is cocontinuous with the SEBS matrix. In Figure 1(c), when the stretched film is cooled to room temperature and solidifies, elastic recovery of the SEBS matrix is restricted by the stacked fibril phase so that the film remains thin. Thus, the SEBS matrix phase gives high gas permeability while the polyolefin phase gives a stable thin film.

Fabrication of a polymer blend film consisting of ethylene–propylene rubber (40 wt %) and polypropylene (60 wt %) with a cocontinuous morphology was previously reported,[15] in which network-like microlayers of ethylene–propylene rubber were formed and stacked in the film thickness direction. The film exhibited an anisotropic thermal expansion coefficient that was much lower in the film plane than in the film thickness direction. This was because the co-continuous structure decreased the molecular mobility of the ethylene–propylene rubber chains. However, there have been no reports on the use of this method to produce thin dense films with high gas permeability.

In the present study, we used MK Resin (Dainihon Plastics, Tokyo, Japan), which is a commercially available polymer blend material consisting of three constituents: SEBS as a thermoplastic elastomer, and poly(ethylene-*co*-ethylacrylate) (EEA) and poly(ethylene-*co*-propylene) (EPP) as polyolefin components. This will henceforth be referred to as MK polymer. MK polymer can be subjected to melt processing (press molding, blow molding, or T-die extrusion) and hot stretching. To determine the optimal composition for achieving the morphology control shown in Figure 1, the isothermal crystallization behavior of two MK-polymer materials, MK-2F and MK-5F, was compared. Aggregated spherulites size of polyolefin phase in MK-2F was much smaller than those in MK-5F. The large crystal size in this polyolefin matrix leads to low gas permeability. Then MK-2F was preferable. Other factor for optimal condition was degree of elastic recovery of SEBS phase. For MK polymers with a much higher fraction of SEBS than polyolefin, a large amount of elasticity recovery of the SEBS phase would be expected following the drawing process, making it difficult to produce thin dense films. From these criteria, optimal polymer was MK-2F.

Blow-molded films prepared using MK-2F were uniaxially hot stretched along the MD (machine direction) and cooled to room temperature. The morphology of the stretched films was observed by transmission electron microscopy (TEM) and their viscoelastic properties were evaluated by dynamic mechanical spectroscopy. The relation between the morphology of the stretched film and its viscoelastic properties during stretching will be discussed. In the resulting films, the dispersed polyolefin phase formed a 3D-network structure which constrained the elastic recovery of the SEBS

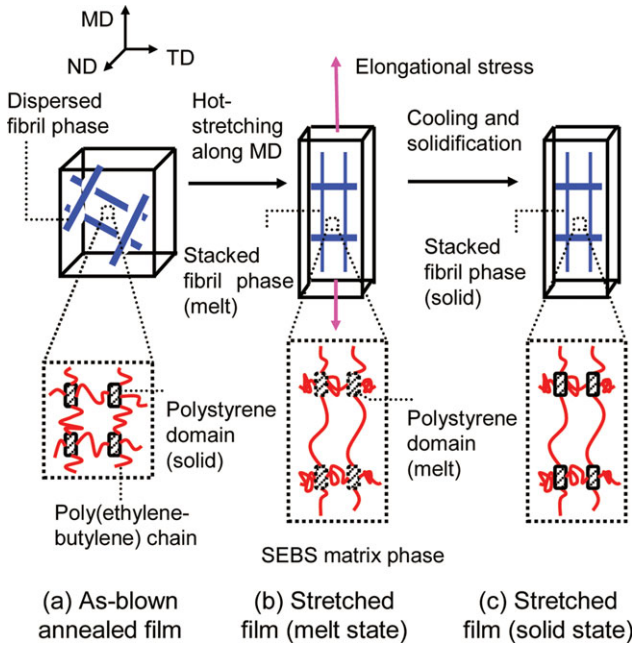

Figure 1. Concept of morphology control in a polymer blend film. [Color figure can be viewed in the online issue, which is available at wileyonlinelibrary.com.]

Table II. Composition of Constituents in MK-2F and MK-5F

	Composition (wt % of constituents)		
MK polymer	SEBS	EEA	EPP
MK-2F	50	30	20
MK-5F	20	40	40

Composition and structure were obtained by C^{13} NMR and H^1 NMR analysis of MK polymer pellets.

matrix phase. The presence of this network structure was a key factor in forming the thin dense films.

EXPERIMENTAL

Polymer Material

As mentioned above, commercially available MK-2F and MK-5F (Dainihon Plastics, Japan) were used as the MK polymer. Both consist of SEBS, EEA, and EPP, but with different proportions of each constituent. The composition of constituents, the chain structure of the constituents, and the thermal characteristics obtained by differential scanning calorimetry (DSC) measurements are shown in Tables II–IV, respectively.

Preparation of As-Blown Annealed Film

The as-blown film was prepared using the film-blowing process shown in Figure 2(a). MK polymer pellets were melted with a melt extruder (EXU-50, Placo, Japan) at 190°C. The polymer melt was well mixed with a screw (diameter 50 mm, $L/D = 28/1$, barrier type) attached to the extruder and the melt was extruded from a slit nozzle (diameter 75 mm, slit width 0.8 mm). The extruded polymer melt formed a cylindrical shape. As shown in Figure 2(a), the polymer melt was stretched in the machine direction (MD) and expanded in both the radial direction (ND) and the circumferential direction [equivalent to the transverse direction (TD) in Figure 2(a)] due to pressure of the film-blowing airflow on the inner side of the polymer melt flow. After the polymer melt flowed, it was quenched by cooling air and solidified at the freeze line as a solid polymer film. The solid polymer film was continually wound and reeled off from the melt extruder. The screw rotation speed was 53 rpm, the polymer extrusion rate was 18 kgh^{-1} and the film was wound at a rate of 6.5 m min^{-1}. The blow ratio was MD/TD = 2/1. The as-blown film (thickness 110 μm) had a cylindrical shape [Figure 2(b)], and was cut along the MD to obtain the rectangular film shown in Figure 2(c). The as-blown film was then annealed for 16 h at 115°C (close to the T_g of the polystyrene domains) to achieve a uniform orientation of the polystyrene domains in the SEBS matrix under tension-free conditions, and was subsequently cooled to room temperature; this is referred to as the as-blown annealed film.

Preparation of Stretched Films

Stretched films were produced using the method shown in Figure 3. As shown in the set-up for stretching, both ends of an as-blown annealed film (110 × 85 mm^2, thickness 110 μm) were clamped with the clamp holder of Tensilon tester (Orientec RTC-1210A, Toyo Seiki Seisaku-sho, Japan) and subjected to uniaxial stretching in the MD at a hot stretching temperature of 120°C; the stretching area was 50 mm (MD) × 85 mm (TD) and the stretching rate was 20 mm min^{-1}. After the film was stretched, its ends were clamped by the clamp holder for 5 min. The door of the heating box of Tensilon tester was then opened and the inner area of the tester was exposed to atmosphere. The film was cooled to room temperature (25°C) while still clamped, and it was then removed from the clamp holder; this is referred to as the stretched film. The stretching ratio K for uniaxial stretching is defined by eq. (1)

$$K = d_0/d_1 \tag{1}$$

where d_0 and d_1 are the thicknesses of the as-blown annealed film and the stretched film, respectively.

Characterization

Isothermal crystallization of MK-2F and MK-5F was investigated using the following procedure. Pressed films (thickness = 150 μm) were prepared by pressing the polymer pellets between two cover glasses at 190°C on a hot plate (Mettler FP-5). The specimens were melted at 200°C for 15 min on the hot plate (to erase their thermal history), cooled to the desired crystallization temperature T_c at 25°C min^{-1} and then crystallized until full solidification occurred. The termination of crystal growth was observed using a polarized optical microscope (Olympus BH-2 PLM) with crossed polarizers, combined with a Polaroid camera. Crystal growth was seen to have almost stopped after 300 min.

The morphology of the MK polymer pellet, as-blown annealed film, and stretched films were observed using TEM (H-8000, Hitachi, Japan, accelerating voltage 200 kV) with ultrathin sections stained with RuO_4. Sample sections (1–2 mm^2, 10-μm thick) were cut from a block of the sample and exposed to RuO_4 vapor generated from a RuO_4-water solution (0.5 wt % solution, Polysciences, USA) at 40°C for 15 min. The exposed section was embedded in Spurr's epoxy resin[16] and hardened

Table III. Chain Structure and Relative Fraction of Constituents

Constituent	Chain structure	Relative fraction (mol %)
SEBS	Polystyrene-block-poly(ethylene butylene)-block-polystyrene triblock copolymer	Styrene/(ethylene butylene) 7/93; ethylene/butylene 75/25
EEA	Ethylene-ethylacrylate random copolymer	Ethylene/ethylacrylate 96/4
EPP	Ethylene-propylene random copolymer	Ethylene/propylene 2/98; polypropylene tacticity: mm/mr/rr 95.9/2.7/1.4

Composition and structure were obtained by C^{13} NMR and H^1 NMR analysis of MK polymer pellets.

Applied Polymer SCIENCE

Table IV. Thermal Properties of Constituents in MK Polymer

	Glass transition	Melting	
Constituent	T_g (°C)	T_r (°C)	T_m (°C)
SEBS			
poly(ethylene/butylene)	−42	−50–32	16
Polystyrene	70		
EEA	−120	35–107	94
EPP	0	107–162	151

DSC measurement conditions: sample pellets were cooled to −150°C and then heated to 180°C at a heating rate of 10°C min^{-1}. T_g = glass transition temperature, T_r = temperature range from the start to end of melting, T_m = melting point.

for 1 day at 60°C. The embedded stained section was cooled with liquid nitrogen and ultrathin sections (ca. 70-nm thick) were sliced using an ultramicrotome (Reichert Scientific Instrument, Germany). Magnification level (scale bar) of each TEM image (Figures 5, 6, 9, 10 in Results and Discussion section) was 0.1, 0.5, 0.5, and 0.1 μm, respectively.

The viscoelastic properties of the sample films were measured as follows. The storage modulus E', loss modulus E'', and tan δ ($= E''/E'$) were measured using a dynamic mechanical spectrometer (DMS-200, SII Nanotechnology, Japan) with tensile mode along the MD and TD of the sample films. Both ends of the film were clamped with the clamp holder of the measurement system and the film was heated from −150 to 150°C at a rate of 2°C min^{-1} and the viscoealstic measurement was done. After the measurement, the film was held at 150°C for 30 min and then cooled to 25°C. The film was then removed from the measurement system and its dimensions were measured. Other measurement parameters were as follows: frequency, 10 Hz; mode, stretching deformation; sample film size in set-up, 10 mm (length) × 8 mm (width). In MD measurement, length direction was MD and width direction TD. On the other hand, in TD measurement, length direction was TD and width direction MD. In both measurements, difference was only the stretching direction of the sample film. In generally, in linear viscoelastic region, strains are within 1% of initial sample length.[13,14] In this experiment, strain amplitude was set at ±0.5% of initial sample length. The number of specimens evaluated for each sample was five. Measurement accuracy was ±5% for each E', E'' data.

Stress strain curve for as-blown annealed film was measured by Tensilon tester (Orientec RTC-1210A, Toyo Seiki Seisaku-sho, Japan) along MD at 25–140°C. The stretching area was 10 mm (MD) × 5 mm (TD) and the stretching rate was 10 mm min^{-1}.

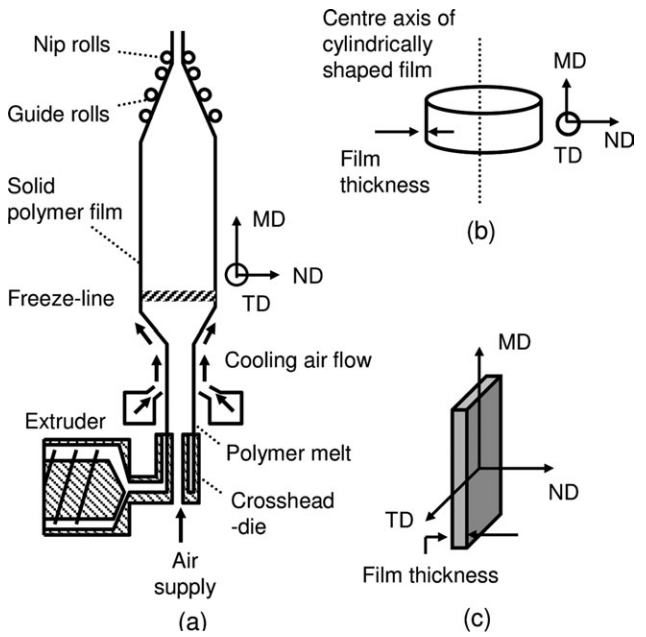

Figure 2. As-blown film preparation method. (a) Film-blowing process, (b) as-blown film (cylindrical shape), and (c) sample film cut from the cylindrically shaped film. MD = machine direction, TD = transverse (to machine) direction, and ND = film thickness direction.

RESULTS AND DISCUSSION

Isothermal Crystallization of MK-2F and MK-5F

The isothermal crystallization behavior of MK-2F and MK-5F was compared using polarized optical microscopy. Micrographs obtained at the termination of the crystallization process are shown in Figure 4(a, b) for MK-2F and MK-5F, respectively. In MK-5F, the polyolefin (EEA+EPP) became the matrix phase and grew to form large aggregated spherulites, clearly observed as bright areas in Figure 4(b). The SEBS, corresponding to the dark areas, was dispersed within the polyolefin matrix. The large

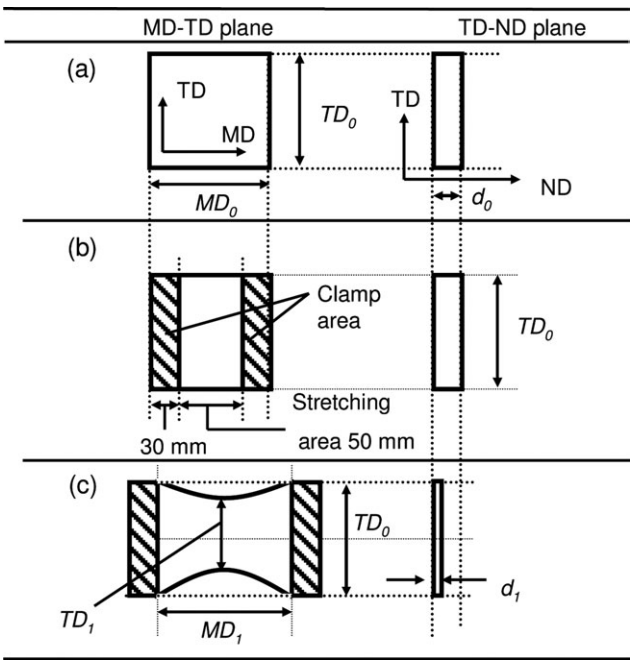

Figure 3. Preparation of uniaxially stretched film. (a) As-blown annealed film (MD_0 = 110 mm, TD_0 = 85 mm, d_0 = 0.11 mm), (b) set-up for stretching, with clamped area indicated by crosshatching, (c) stretched film, e.g., MD_1 = 205 mm, d_1 = 0.025 mm, and TD_1 = 70 mm at a stretching temperature of 120°C, K = 4.1.

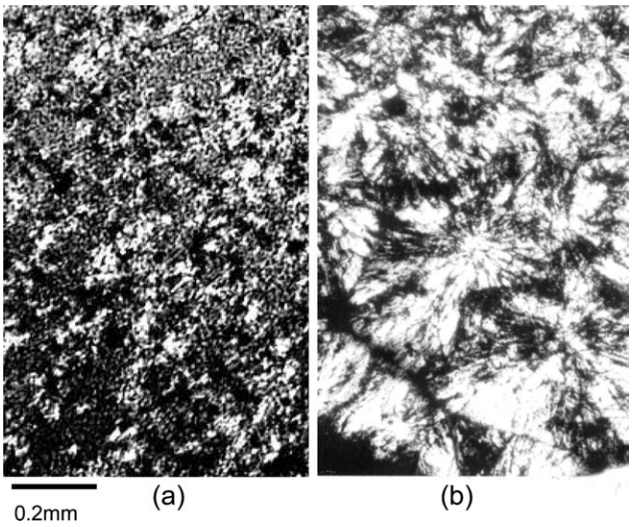

Figure 4. Polarized optical micrographs of (EEA + EPP) spherulites (bright regions) at endpoint of isothermal crystallization from the melt (200°C): (a) MK-2F at a crystallization temperature of $T_C = 125$°C for 300 min; (b) MK-5F at $T_C = 125$°C for 300 min.

crystal size in this polyolefin matrix leads to low gas permeability. On the other hand, as seen in Figure 4(a), the polyolefin (EEA + EPP) in MK-2F became the dispersed phase and its spherulite crystals were much smaller than those in MK-5F.

For MK polymers with a much higher fraction of SEBS than polyolefin, a large amount of elasticity recovery of the SEBS phase would be expected following the drawing process, making it difficult to produce thin dense films. However, it has been reported that for polymer blends with a SEBS/HDPE ratio in the range of 60/40 to 50/50 (wt %), a bi-continuous structure is easily obtained with a high degree of phase continuity.[17] Therefore, the composition of MK-2F with SEBS/polyolefin = 50/50 (wt %) is considered to make it suitable for the production of thin dense membranes.

The following sections describe the morphology of a blow-molded film prepared from MK-2F that was uniaxially hot stretched along the MD, and a comparison with the morphology of an MK-2F pellet. The viscoelastic properties of the stretched films during stretching are also discussed.

Morphology of MK-2F Pellet

TEM images of the phase-separated structure of an MK-2F pellet are shown in Figure 5(a, b). In these figures, the bright regions represent the dispersed phase of the EEA and EPP mixture, while the dark regions correspond to the SEBS matrix phase. In Figure 5(a), the dispersed phase is either in the form of stretched fibers (fibril-like dispersed phase) oriented along the MD or in the form of droplets (droplet dispersed phase). The fibril-like dispersed phase might have become necked and broken into the droplet dispersed phase due to the extrusion force during melt-extrusion of the pellet. Figure 5(b) shows that the polystyrene domains are cylindrical in shape (diameter 200 Å) and their axes are oriented along the MD, i.e., the extrusion direction of the MK polymer pellet. The bright narrow regions (50–100 Å wide) between the polystyrene domains are areas where EB chains are present.

Thus, the MK-2F polymer pellet had a phase-separated structure, with a SEBS matrix phase and a dispersed phase comprising a mixture of EEA and EPP with a fibril-like or droplet shape.

As-blown Annealed Film of MK-2F

Morphology. TEM micrographs of the as-blown annealed film in the MD-ND and TD-ND planes are shown in Figure 6(a, b), respectively. The morphology resembles that of the pellet. The dark regions represent the SEBS matrix phase and the bright regions the dispersed phase of the EEA and EPP mixture that forms fibril-like or droplet shapes. Hereafter, the dispersed

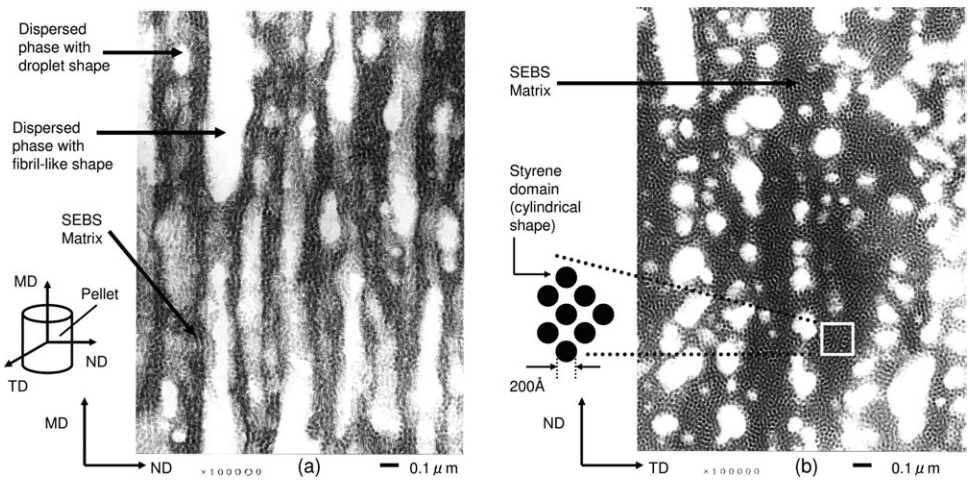

Figure 5. Cross-sectional TEM micrographs of MK-2F pellet. (a) is in the MD-ND plane, while (b) is in the TD-ND plane. Polystyrene domains (cylindrical shape) in the SEBS matrix are stained dark with RuO_4 vapor. Ru metal coordinates with the double bond of polystyrene as an oxidation site.[18,19] EB chains appear as bright areas between the polystyrene domains. MD indicates the machine direction, which is parallel to the extrusion direction, TD the transverse direction to the MD, and ND the direction normal to both MD and TD.

Applied Polymer SCIENCE

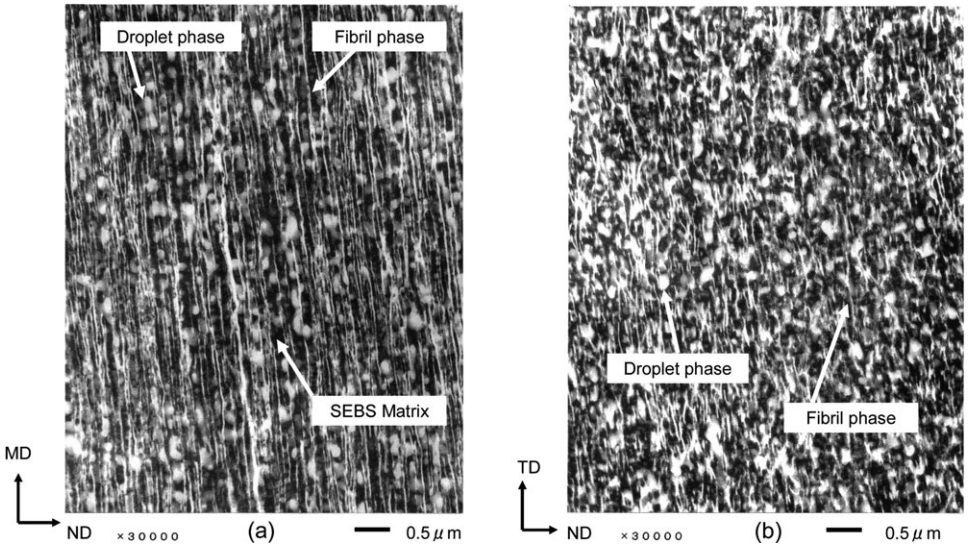

Figure 6. TEM micrographs of as-blown annealed film of MK-2F in the (a) MD-ND and (b) TD-ND planes.

phase will be referred to as the fibril phase or fibril and the droplet phase or droplet.

From the morphology of the as-blown annealed film, the direction of stress during the film blowing process was estimated. In the MD-ND plane, the fibril phase was stretched in the MD and its width was very small (<0.05 μm) compared with that of the pellet (0.1–0.2 μm). From this result, the melt tension applied to the polymer flow during the film-blowing process was higher than that during the pellet extrusion process. In addition, the fibrils were also slightly inclined towards the ND. On the other hand, in the TD-ND plane, the fibril phase was stretched in the TD and was also slightly inclined toward the ND. The degree of orientation in the TD is not so high compared with that in the MD. In the 3D space of MD-TD-ND, the fibril phase was stretched mainly in the MD, with a slight inclination towards the TD and ND, which suggests that the stress applied to the melt during the film-blowing process was mainly along the MD and the polymer flowed in these directions.

Kotaka et al. reported[20,21] that when SEBS underwent elongational flow, both the cylindrical styrene domains and EB chains were oriented along the direction of elongational stress in the melt state. They also showed that after the melt flow was rapidly quenched to a solid polymer with ice water, the orientation of both the polystyrene domains and EB chains remained.

During the film-blowing process in the present study, it could also be estimated that the EB chains, with both ends connected to polystyrene domains, were stretched along the polystyrene domain orientation and this stretched state was rapidly quenched at the freeze line. Therefore, in the as-blown annealed film, EB chains would be stretched mainly in the MD before the freeze line (Figure 2). After quenching, the orientation of the EB chains would be fixed and the chains would remain in a state of tension.

Stress-Strain Curve

The stress-strain curve for the as-blown annealed MK-2F film measured along the MD is shown in Figure 7. In the temperature range of 25–60°C, strain hardening was observed in the high-strain region (>400%). On the other hand, in the range of 80–140°C, no such strain hardening occurred. At temperatures of 120–140°C, the yield stress was reduced in the low-strain region (strain of <20%) and high elongation to break (>1200%) was achieved because of the collapse of the styrene network structure and the partial melting of the polyolefin phase. Therefore, the optimum stretching temperature was 120–140°C, and in the present experiment, stretching was carried out at 120°C.

Morphology of Stretched Films

After stretching along the MD at 120°C and cooling to room temperature, the stretching ratio K based on eq. (1), the film length ratio (MD_1/MD_0), and the film width ratio (TD_1/TD_0) are plotted versus the set value of the stretching ratio R in Figure 8(a, b). Both the stretching ratio K and the film length ratio (MD_1/MD_0) increased linearly with R, which indicates that elastic recovery could be constrained for this stretching process. In the TD, the width of the stretched film, TD_1, decreased linearly with increasing R, although the change was small [Figure 8(b)].

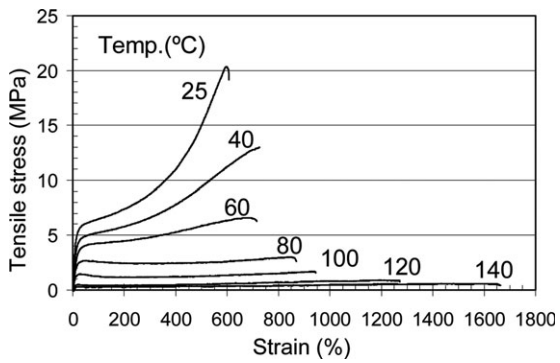

Figure 7. Stress–strain curve for as-blown annealed film along MD. Strain is defined as $\Delta MD/MD_0$, where ΔMD is the stretched length from MD_0 along the MD. The stretching rate was 20 mm min^{-1}.

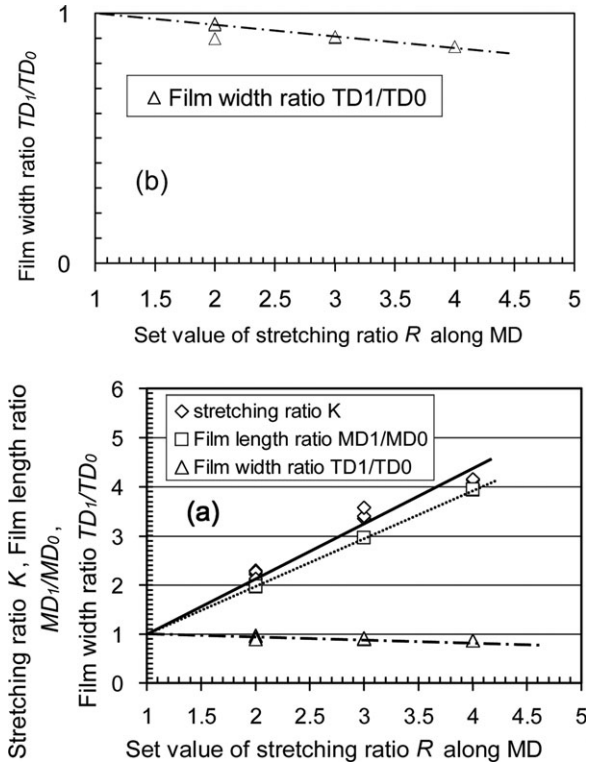

Figure 8. Dimensional changes of stretched films following stretching at 120°C along the MD and cooling to room temperature. (a) shows the stretching ratio K, film length ratio MD_1/MD_0, and film width ratio TD_1/TD_0. (b) is an expanded view of the change in TD_1/TD_0 during stretching. The set value of the stretching ratio is given by $R = (MD_0 + \Delta R)/MD_0$, where ΔR is the movement distance from the initial position of the crosshead in the Tensilon tester. The stretching rate was the same as in Figure 7. MD_0 and MD_1 are the lengths of the as-blown annealed film and the stretched film, respectively. TD_0 and TD_1 are the widths of the as-blown annealed film and the stretched film, respectively. The stretching ratio K is defined by eq. (1). The straight lines drawn on the graphs represent linear trend lines.

TEM micrographs of the stretched films of MK-2F are shown in Figures 9(a–d) and 10(a–d). Figure 9(a, b) is for $K = 2.1$ in the MD-ND plane and TD-ND plane, respectively. Figure 9(c, d) is for $K = 4.1$ in the MD-ND plane and TD-ND plane, respectively. Figure 10(a, b) is higher magnification TEM images for $K = 2.1$ and Figure 10(c, d) is for $K = 4.1$. The morphology in these micrographs indicates that the dispersed phase is highly stretched in the MD and TD compared with that of the as-blown annealed film. In the MD-ND plane of the stretched films, the fibril phase is undulated along the MD for $K = 2.1$ [Figures 9(a) and 10(a)] and the fibril phase is more highly stretched and becomes quite thin (width 0.03–0.04 μm) for $K = 4.1$, as shown in Figures 9(c) and 10(c). In the TD-ND plane [Figures 9(d) and 10(d)], the fibril phase becomes quite thin for $K = 4.1$. The droplet phase is stretched in both the MD and TD and the shape becomes highly distorted with increasing K [Figures 9(a–d) and 10(a–d)]. From Figure 9(a–d), with increasing K, a very interesting morphology for the dispersed phase was observed, in that the droplet phase was stacked with the fibril phase. This is because the film thickness decreased with increasing stretching ratio and the distance between the fibril and droplet phases in the thickness direction decreased until the fibril phase was finally stacked with the droplet phase. At high stretching ratios (e.g., $K = 4.1$), the stacked dispersed phase formed a network-like structure as shown in Figures 10(c, d). At high stretching ratios, in addition to this morphology, the cylindrical polystyrene domains were oriented mainly in the MD.

Based on these TEM results, a schematic representation of the proposed morphology change for the dispersed phase during the uniaxial stretching process is shown in Figure 11. As K increased, both the film thickness and the distance between the fibril and droplet phases decreased. At $K = 4.1$, the two phases were stacked and a network-like structure was formed. Highly elongated droplets acted as crosslinking points in the network structure. In addition, the SEBS was also stretched in the MD and this deformation remained following cooling to room temperature due to the presence of the network structure. Based on Figure 11, the morphology control concept in Figure 1 is thus verified. In the next section, the change in the molecular motion of the SEBS matrix during stretching is examined using viscoelastic measurements.

Viscoelastic Properties of MK-2F Films

Measurement Results Along the MD. Viscoelastic measurement results for the as-blown annealed film and stretched films along the MD are shown in Figure 12(a). From viscoelastic theory, the work done on polymer chains by an external force in viscoelastic measurements is dissipated in the form of thermal energy by friction between the chains. The E'' curve shows the dissipated energy loss. When the temperature increases to around the glass transition temperature, the molecular mobility of the chains increases; therefore, the friction between the chains increases, which results in an increase in energy loss. On the other hand, when the temperature is much higher than the glass transition temperature, the chains move easily due to a transition to a rubbery state; therefore, the friction decreases and the energy loss decreases. In this way, the energy loss becomes maximized around the glass transition temperature. In Figure 12(a), the viscoelastic property E' is the Young's modulus of the polymer material. Near the glass transition temperature for the material, E' decreased gradually. At the glass transition temperature, E' rapidly decreased in a stepwise fashion and above the glass transition temperature, E' deceased gradually.

The viscoelastic data for the as-blown annealed film along the MD indicates that the EB chains have a dominant effect on the mechanical property E'. In Figure 12(a), the loss modulus E'' curve for the as-blown annealed film has four peaks at −125, −50, 0, and 70–90°C, which correspond to the glass transition temperatures of EEA, EB, EPP, and the polystyrene domains, respectively. The glass transition temperatures indicated by the E'' curve are in good agreement with the thermal properties data listed in Table IV. When the temperature was higher than −50°C, E' decreased remarkably and the increase in EB chain mobility mainly contributed to the deformation of the film. Hereafter, EB chains with high molecular mobility after the

Applied Polymer SCIENCE

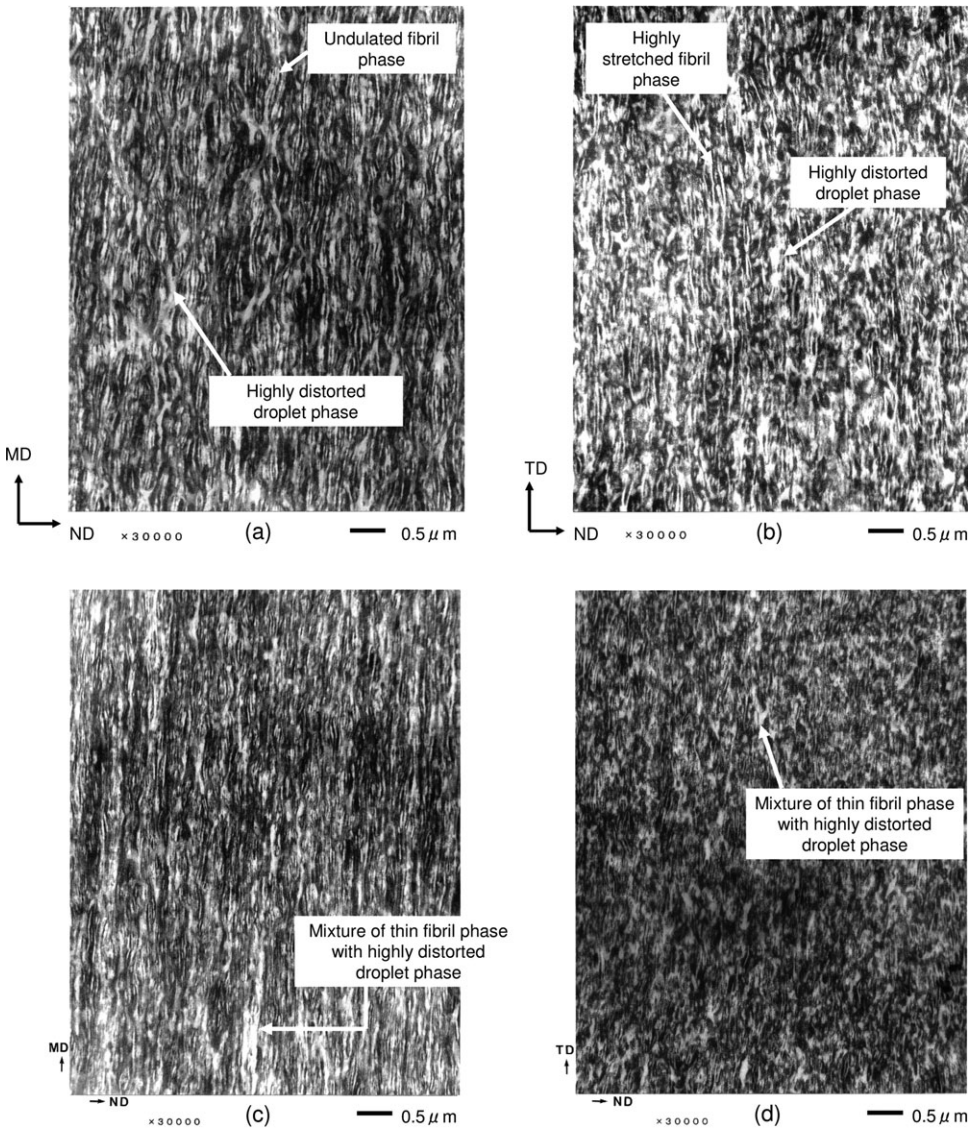

Figure 9. TEM micrographs of the stretched film of MK-2F. (a and b) are for $K = 2.1$ and a stretching temperature of 120°C. (a) is in the MD-ND plane and (b) is in the TD-ND plane. (c and d) are for $K = 4.1$ at 120°C. (c) is in the MD-ND plane and (d) is in the TD-ND plane.

glass transition followed by a transition to a rubbery state are referred to as EB rubber chains. At temperatures higher than 70°C, the polystyrene domains underwent a glass transition and the physical crosslinked structure of the domain collapsed. Because of this collapse, the entire SEBS matrix phase became more susceptible to deformation and E' decreased rapidly. At temperatures higher than 120°C the deformation of the film became significant, so that it was difficult to measure E'.

The viscoelastic properties of the stretched film ($K = 4.1$, 120°C) were compared with those of the as-blown annealed film. At temperatures higher than −50°C, E' for the stretched film ($K = 4.1$) was slightly higher than that for the as-blown annealed film, although at approximately the same level. In the vicinity of 70°C, E' for the stretched film rapidly decreased stepwise, which was similar to the case for the as-blown annealed film. The E'' curves for the as-blown annealed film and the stretched film ($K = 4.1$) overlapped, which indicated that the glass transition temperature for each constituent did not change due to stretching. From the dimensional change of the stretched film (Figure 8), the EB rubber chains in the stretched films were further stretched along the MD compared to the case for the as-blown annealed film, suggesting that the mobility of the chains along the MD might have decreased. There is a possibility that the stretched EB rubber chains along the MD were relaxed as the temperature was increased during the viscoelastic measurement.

Viscoelastic Properties Along the TD. The viscoelastic properties of the as-blown annealed film and stretched films ($K = 2.1$, 3.4, and 4.1) along the TD are shown in Figure 12(b). At temperatures higher than −50°C, E' declined rapidly for both the as-blown annealed film and the stretched films. As the stretching ratio was increased ($K = 2.1$, 3.4, and 4.1), the decline in E' became more significant. Therefore, it was considered that the EB rubber chains in the stretched films were relaxed in the TD

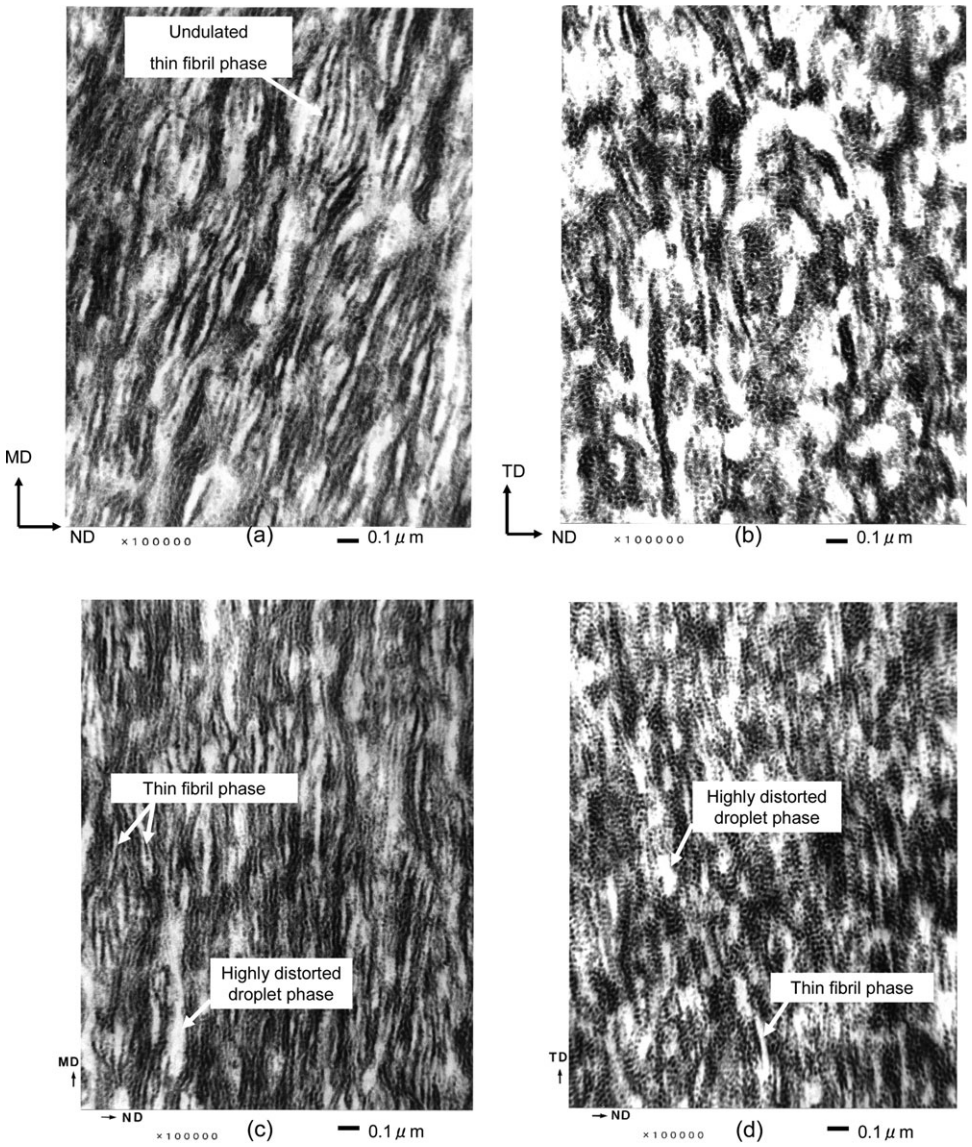

Figure 10. TEM micrographs of the stretched film of MK-2F ($K = 2.1$, 120°C) at higher magnification. (a) is in the MD-ND plane and (b) is in the TD-ND plane. (c and d) are for $K = 4.1$ at 120°C. (c) is in the MD-ND plane and (d) is in the TD-ND plane.

compared with the case for the as-blown annealed film, and the molecular mobility of the EB rubber chains along the TD increased with K. The stretched films became contracted in the TD as K increased and stress was stored. The rapid increase in tan δ with stretching was due to the decline in E'. Therefore, in the stretching process, the EB rubber chains became contracted in the TD and were gradually relaxed along the TD with increasing stretching ratio; thus, the molecular mobility of the EB rubber chains increased in the TD.

After the viscoelastic measurement along the TD with heating from −150 to 150°C and cooling to 25°C, the stretched films contracted in the MD and expanded in the TD. This tendency was more remarkable as the stretching ratio increased. Before the measurement, the stretched film had elongated in the MD and contracted in the TD compared with the as-blown annealed film, and residual stress remained in the EB rubber chains. The chains were in a state of tension and this state was maintained by the physical crosslinked structure of the SEBS matrix and the 3D-network of the dispersed phase. During the viscoelastic measurement, when the stretched film was heated to 150°C, the polystyrene domains underwent a glass transition, the physical crosslinked structure of the domains collapsed and the 3D-network structure of the dispersed phase melted. Therefore, elastic recovery occurred and the entire stretched film contracted in the MD.

Deformation Model for the SEBS Matrix

In the as-blown annealed film, the EB rubber chains were stretched in the MD, TD, and ND and were already in a state of tension with low molecular mobility. When the film was stretched in the MD, the EB rubber chains were further stretched in the MD and their molecular mobility further decreased. In contrast, in the TD, perpendicular to the

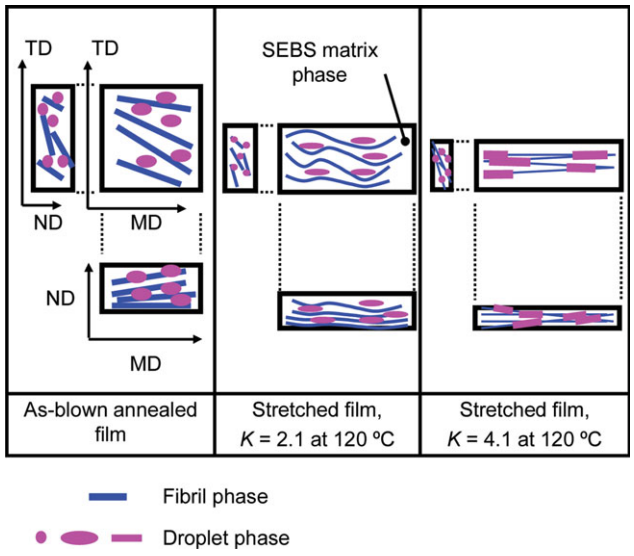

Figure 11. Morphology change of dispersed phase during uniaxial stretching process for MK-2F. [Color figure can be viewed in the online issue, which is available at wileyonlinelibrary.com.]

stretching direction, the EB rubber chains were relaxed upon stretching and their molecular mobility increased.

To understand this anisotropy in molecular mobility with stretching, a model for deformation of the SEBS matrix is presented in Figure 13 as a pattern diagram. In this model, the EB rubber chains in the as-blown annealed film are in a state of tension in the MD, TD, and ND. In the stretched films, the chains are further stretched in the MD, but become contracted in the TD and ND. This contraction in the ND is due to the thickness decrease during stretching.

This model is based on the following assumptions.

1. EB rubber chains have rubber-like elasticity and are capable of affine deformation. In Figure 13, the only area where the EB rubber chains are present is subjected to uniaxial deformation under constant volume. In general, when the Poisson's ratio is 0.50, deformation is considered to be affine.[13,14] In the SEBS polymer, the Poisson's ratio of the EB chain is 0.49.[22] Therefore, it is considered that the EB rubber chains undergo affine deformation. Thus, the volume that the rubber chains occupy becomes invariant and the chains contract in both the ND and TD, and extend in the MD.
2. The polystyrene domains are not deformed. Young's modulus for the polystyrene domains (24 MPa) is larger than that for EB chains (6.4 MPa)[22]; therefore, it can be assumed that the polystyrene domain shape does not change during stretching.
3. The cylindrical polystyrene domains are aligned in the MD with a decreased spacing between neighbors to form a moniliform structure. The moniliform structure was also confirmed from TEM observations [Figures 9(a–d) and 10(a–d)].

In the stretched films, a 3D-network structure of polyolefin phase (Figure 11) was formed, causing the anisotropy in molecular mobility presented in Figure 13 to be maintained. This network structure was a key factor in forming the thin dense films.

In viscoelastic measurement result along MD in Figure 12(a), when temperature was higher than −50°C, E' decreased remarkably in the temperature range of −50 to nearly 70°C and reached in plateau region at about 70°C. The decrease in E' was the result from increase in EB chain mobility and the plateau behavior was the result from glass–rubbery transition of styrene domain in SEBS matrix. The effect of 3D-network structure formed during stretching appeared in the plateau region. The E' value at plateau region became higher with the increase in stretching ratio. This increase in E' value would be due to the formation of 3D-network structure during stretching. The same trend was appeared in Figure 12(b) in TD measurement. Both

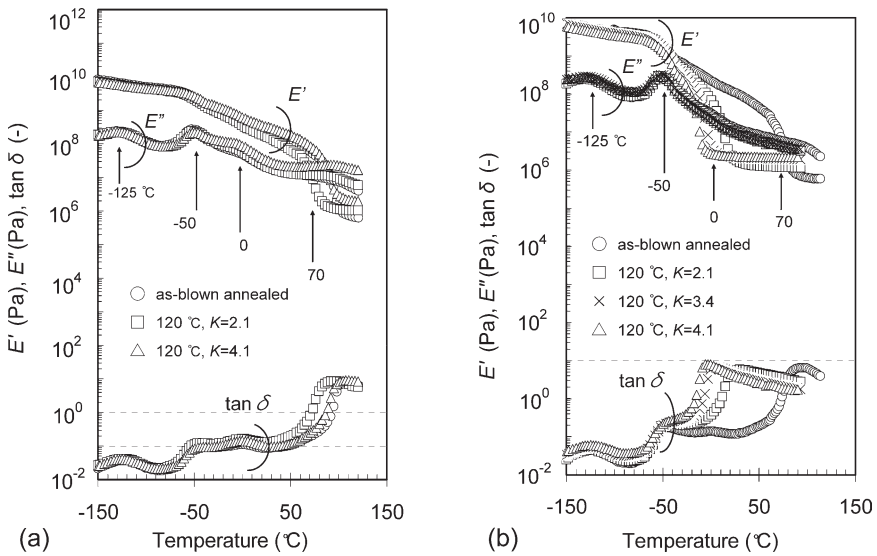

Figure 12. Viscoelastic properties of the as-blown annealed film and stretched films along the (a) MD and (b) TD.

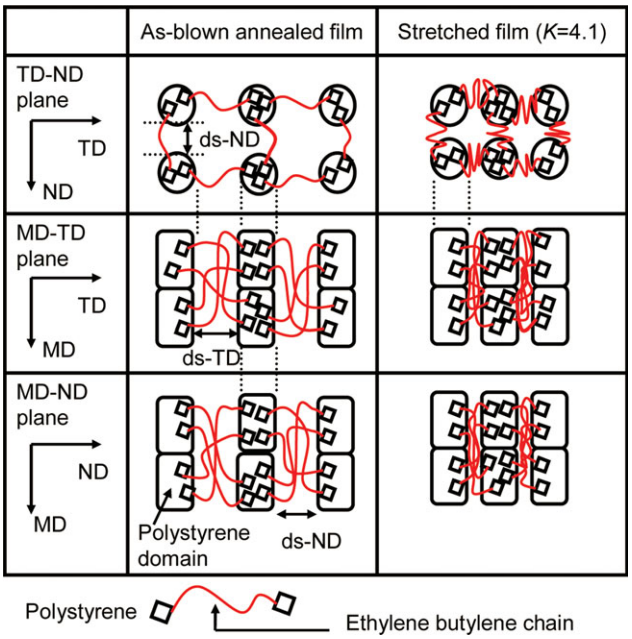

Figure 13. Deformation model for the SEBS matrix under uniaxial stretching. ds-ND and ds-TD represent the distance between neighboring polystyrene domains along the ND and TD, respectively. [Color figure can be viewed in the online issue, which is available at wileyonlinelibrary.com.]

MD and TD viscoelastic measurement results showed the formation of 3D-network structure during stretching.

CONCLUSION

In this study, stretched thin films composed of a thermoplastic elastomer and polyolefins were obtained by uniaxial stretching and cooling to room temperature. In the resulting films, the dispersed polyolefin phase formed a 3D-network structure which constrained the elastic recovery of the SEBS matrix phase. The presence of this network structure was a key factor in forming the thin dense films.

In the as-blown annealed film, the EB rubber chains were stretched in the MD, TD, and ND and were already in a state of tension with low molecular mobility. When the film was stretched in the MD, the EB rubber chains were further stretched in the MD and their molecular mobility further decreased. In contrast, in the TD, perpendicular to the stretching direction, the EB rubber chains were relaxed upon stretching and their molecular mobility increased. To understand this anisotropy in molecular mobility with stretching, a model for deformation of the SEBS matrix was presented.

ACKNOWLEDGMENTS

The authors are grateful to Drs. Jun Nakauchi, Senior Research Fellow, Mitsubishi Rayon and Akira Hasegawa, former Fellow, Mitsubishi Rayon for their encouragement and involvement in discussions concerning data interpretation for this research article, and to Mr. Hideyuki Nakamoto of the Structural Analysis Research Division, Mitsui Chemical Analysis and Consulting Service, for his support during TEM observations.

REFERENCES

1. Endoh, M. In Handoutai Process Kyouhon (in Japanese); SEMI Forum Japan Program Committee, Ed.; SEMI Forum Japan: Tokyo, Japan, **2007**; p 94.
2. Technical Bulletin of Gas Permeability of KRATON Rubber; Shell Chemical Company: Lisle, Illinois, **1995**.
3. Roland, C. M. Polymer Data Handbook; Oxford University Press: New York, **1999**; p 161.
4. Yasuda, H.; Stannet, V. In Polymer Handbook, 2nd ed.; Brandrup, J., Immergut, E. H., Eds.; Wiley-Interscience Publication: New York, **1975**; p 229.
5. Pauly, S. In Polymer Handbook, 4th ed.; Brandrup, J., Immergut, E. H., Grulke, E. A., Eds.; Wiley-Interscience Publication: New York, **1999**; p 543.
6. Michaels, A. S.; Bixler, H. J. J. Polym. Sci. **1961**, *50*, 413.
7. Myers, A. W.; Stannet, V.; Szwarc, M. J. Polym. Sci. **1959**, *35*, 285.
8. Yasuda, H.; Rosengren, K. J. J. Appl. Polym. Sci. **1970**, *14*, 2839.
9. Nagano, T. Permeability Data of Ethylene–Ethylacrylate Copolymer Products; Nippon Unicar Co., Ltd.: Tokyo, Japan. unpublished data (Private Communication), **2004**.
10. McCarthy, R. A. In Encyclopedia of Polymer Science and Engineering; Mark, H. F., Bikales, N. M., Overberger, C. G., Menges, G., Kroschwitz, J. I., Eds.; Wiley: New York, **1989**; Vol. 3, p 421.
11. Holden, G.; Legge, N. R. In Thermoplastic Elastomers, 2nd ed.; Holden, G., Legge, N. R., Quirk, R. P., Shroeder, H. E., Eds.; Hanser Publishers: Munich, **1996**; Chapter 3, p 47.
12. Gergen, W. P.; Lutz, R. G.; Davison, S. In Thermoplastic Elastomers, 2nd ed.; Holden, G., Legge, N. R., Quirk, R. P., Shroeder, H. E., Eds.; Hanser Publishers: Munich, **1996**; Chapter 11, p 297.
13. Ward, I. M.; Sweeney, J. S. An Introduction to the Mechanical Properties of Solid Polymers, 2nd ed.; Wiley: New York, **2004**.
14. Nielsen, L. E.; Landel, R. F. Mechanical Properties of Polymers and Composites, 2nd ed.; Marcel Dekker, Inc: New York, **1994**.
15. Wu, G.; Nishida, K.; Takagi, K.; Sano, H.; Yui, H. Polymer **2004**, *45*, 3085.
16. Spurr, A. R. J. Ultrastruct. Res. **1969**, *26*, 31.
17. Jianming, L.; Pei Lian, M.; Basil, D, F. Macromolecules **2002**, *35*, 2005.
18. Trent, J. S.; Scheinbeim, J. I.; Couchman, P. R. Macromolecules **1983**, *16*, 589.
19. Ohlsson, B.; Tornell, B. J. Appl. Polym. Sci. **1990**, *41*, 1189.
20. Kotaka, T.; Okamoto, M.; Kojima, A.; Kwon, Y. K.; Nojima, S. Polymer **2001**, *42*, 3223.
21. Kobori, Y.; Kwon, Y. K.; Okamoto, M.; Kotaka, T. Macromolecules **2003**, *36*, 1656.
22. Motomatsu, M.; Muzutani, W.; Tokumoto, H. Polymer **1999**, *38*, 1779.